Supporting Information

An effective strategy to obtain near-infrared emission from shoulder to shoulder-type binuclear platinum(II) complex based on fused pyrene core bridged isoquinoline ligands

KaiZhang,[a] Tianyu Wang,[a] Tingwen Wu,[b]* Zhenming Ding,[a]
Qiang Zhang,[a] Weiguo Zhu,[a]* and Yu Liu[a]*

[a] *School of Materials Science and Engineering, Jiangsu Collaboration Innovation Center of Photovoltaic Science and Engineering, Jiangsu Engineering Laboratory of Light-Electricity-Heat Energy-Converting Materials and Applications, National Experimental Demonstration Center for Materials Science and Engineering, Changzhou University, Changzhou 213164, P. R. China*

[b] *Shenzhen CNOOC EnerTech-Marketing Services Co. Ltd. Shenzhen 518067, P. R. China*

E-mail: wutw@cnooc.com.cn

(W. Zhu) zhuwg18@126.com

(Y. Liu) liuyu03b@126.com

Contents

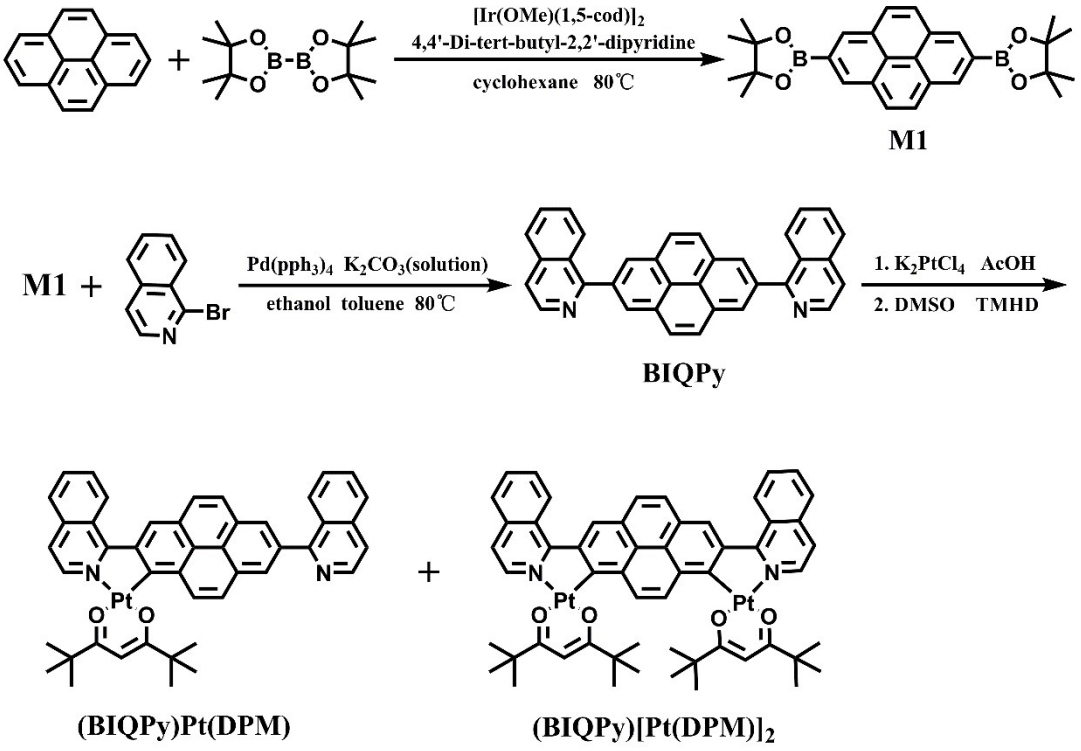

Scheme S1. Synthetic route of platinum(Ⅱ) complexes.

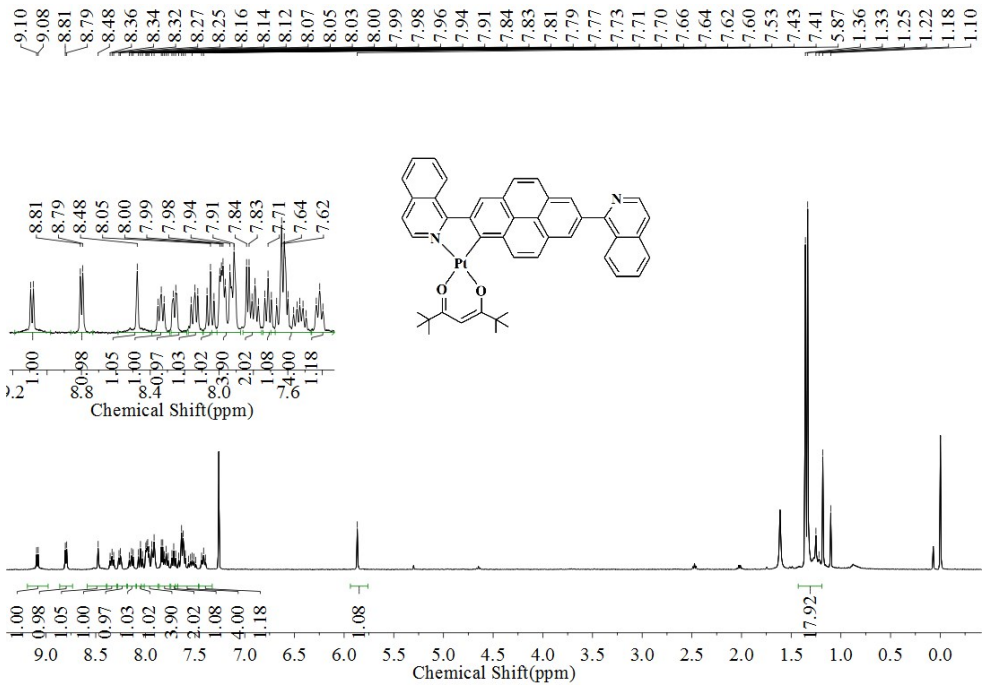

Figure S1. ^{1}H NMR spectrum of (BIQPy)Pt(DPM).

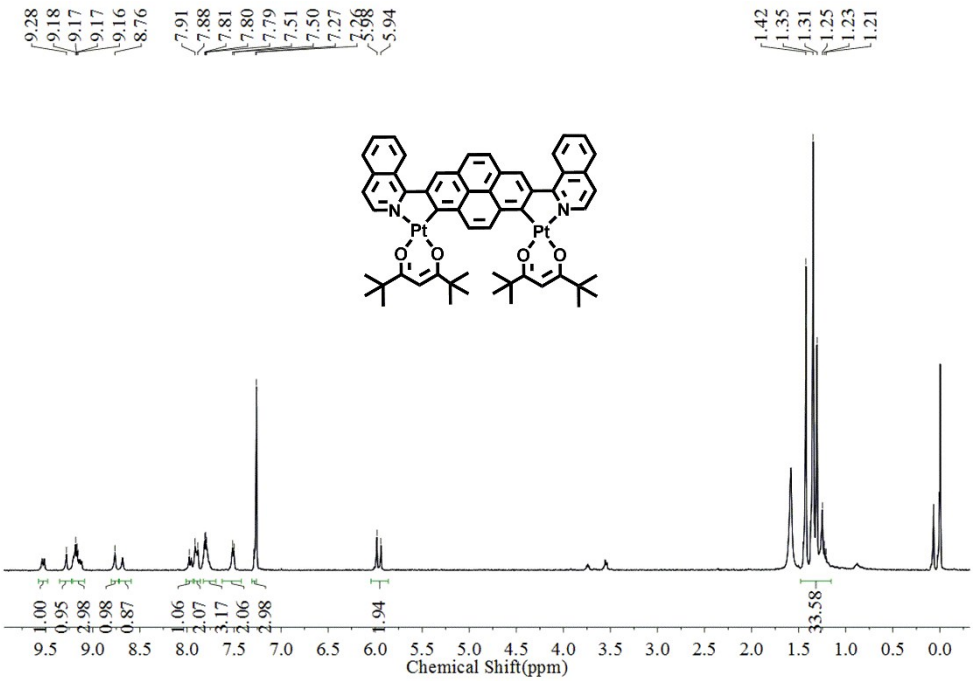

Figure S2. ^{1}H NMR spectrum of (BIQPy)[Pt(DPM)]$_2$.

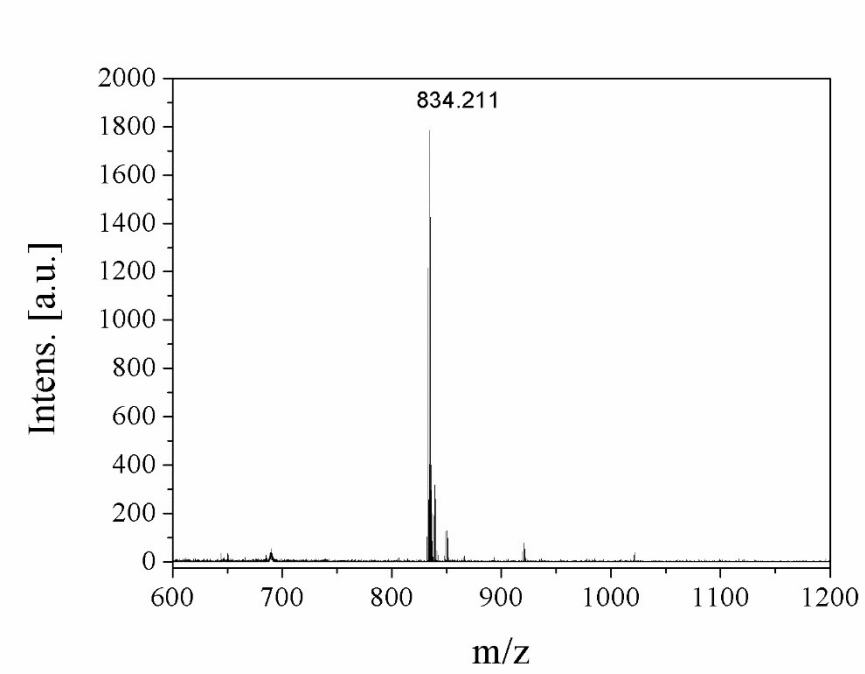

Figure S3. High resolution MS spectrum of (BIQPy)Pt(DPM).

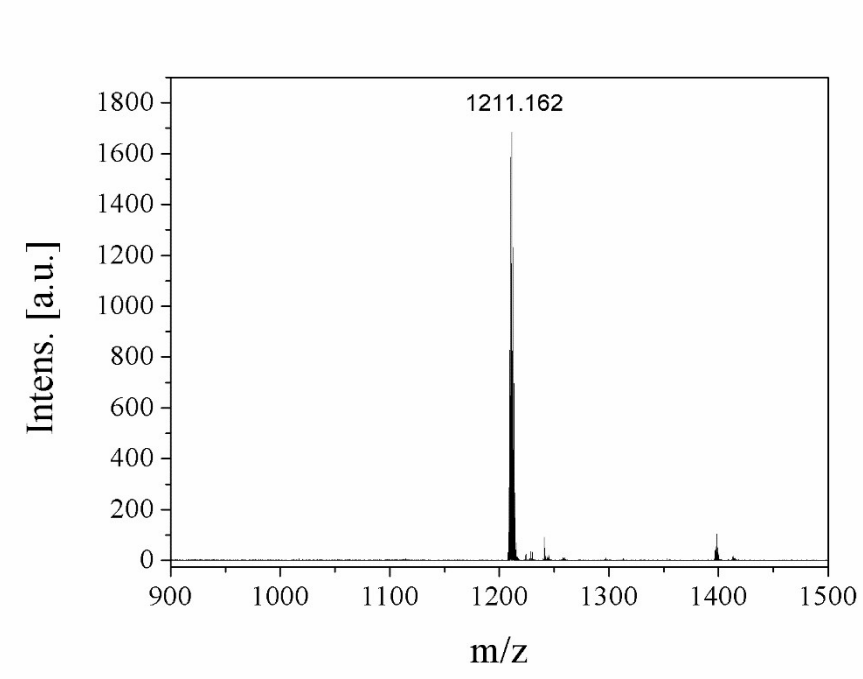

Figure S4. MALDI-TOF MS spectrum of (BIQPy)[Pt(DPM)]$_2$.

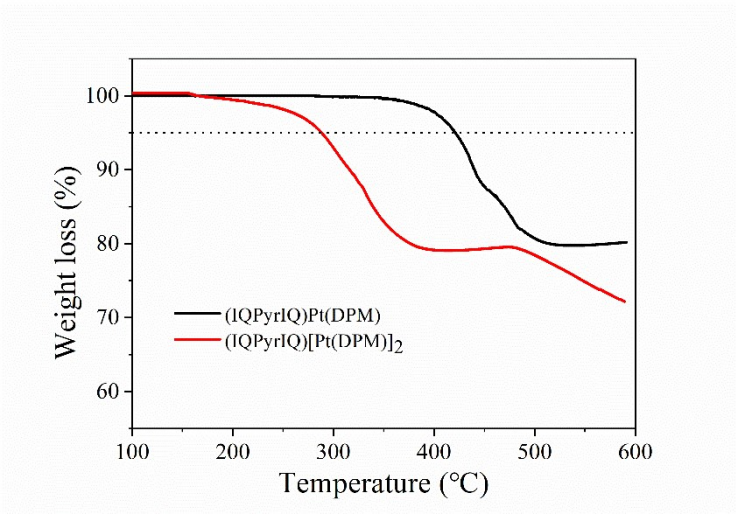

Figure S5. TGA curves of Pt(II) complexes under N_2 with a rate of 20 ^{o}C/min.

.

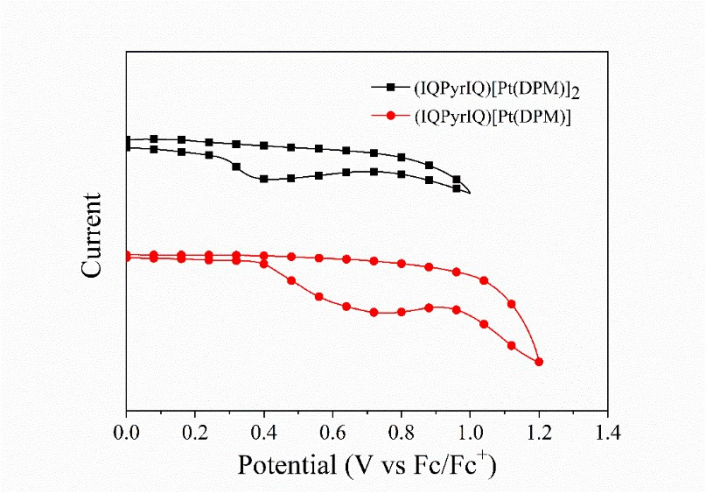

Figure S6. Cyclic voltammograms of Pt(II) complexes in CH_3CN solutions.

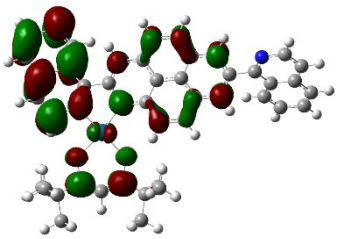	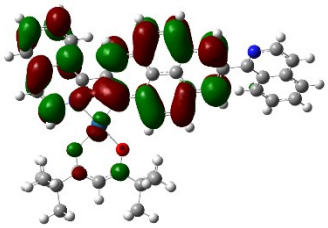	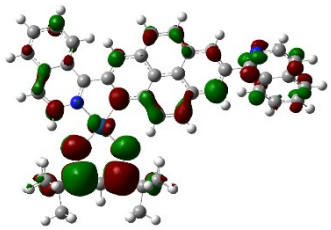
LUMO+4	LUMO+3	LUMO+2
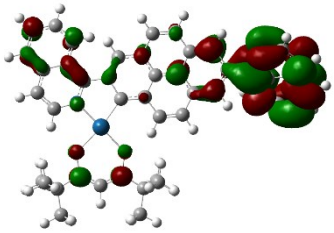	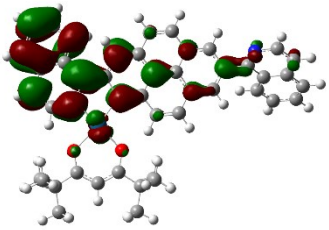	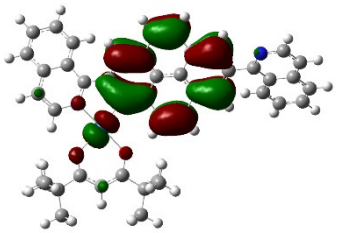
LUMO+1	LUMO	HOMO
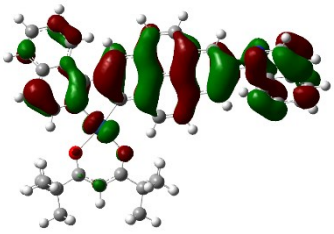	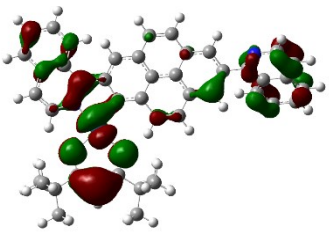	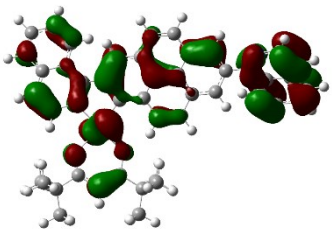
HOMO-1	HOMO-2	HOMO-3
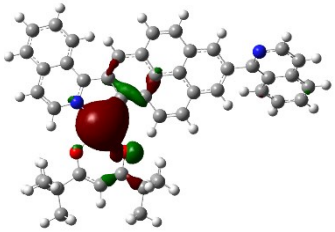	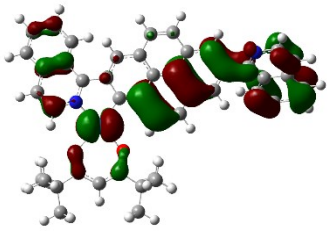	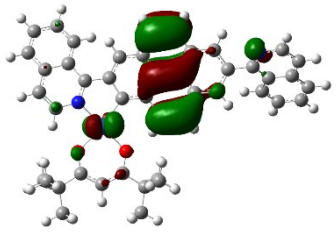
HOMO-4	HOMO-5	HOMO-6

Figure S7. Iso-surface contour plots (iso-value = 0.02) of selected orbitals of model

(BIQPy)Pt(DPM) in the ground state (S_0) geometry.

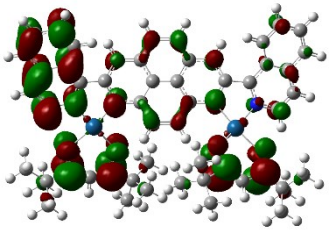	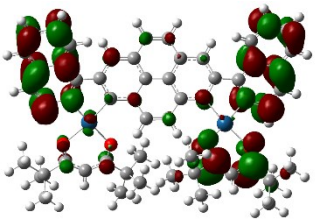	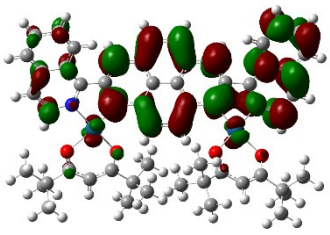
LUMO+4	LUMO+3	LUMO+2
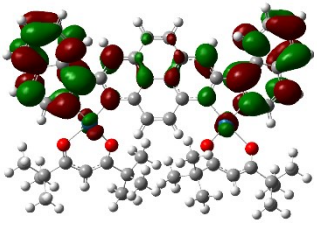	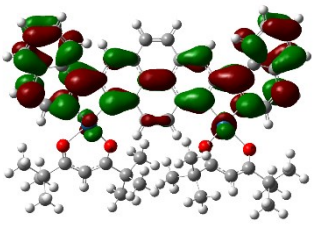	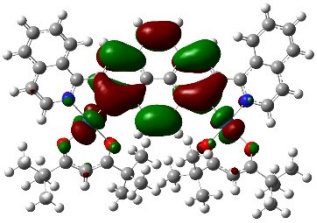
LUMO+1	LUMO	HOMO
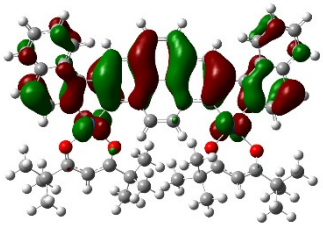	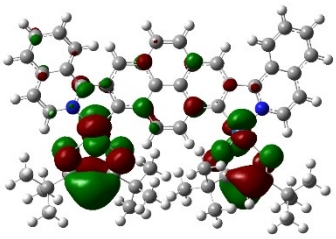	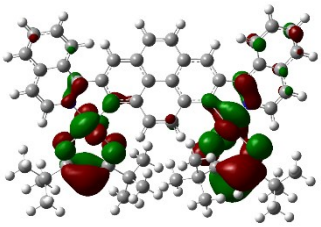
HOMO-1	HOMO-2	HOMO-3
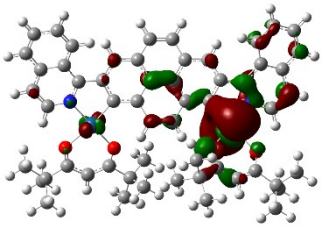	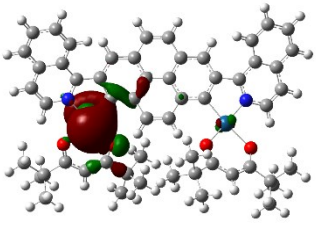	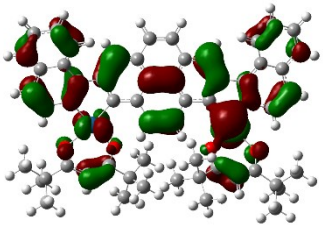
HOMO-4	HOMO-5	HOMO-6

Figure S8. Iso-surface contour plots (iso-value = 0.02) of selected orbitals of model (BIQPy)[Pt(DPM)]$_2$ in the ground state (S_0) geometry.

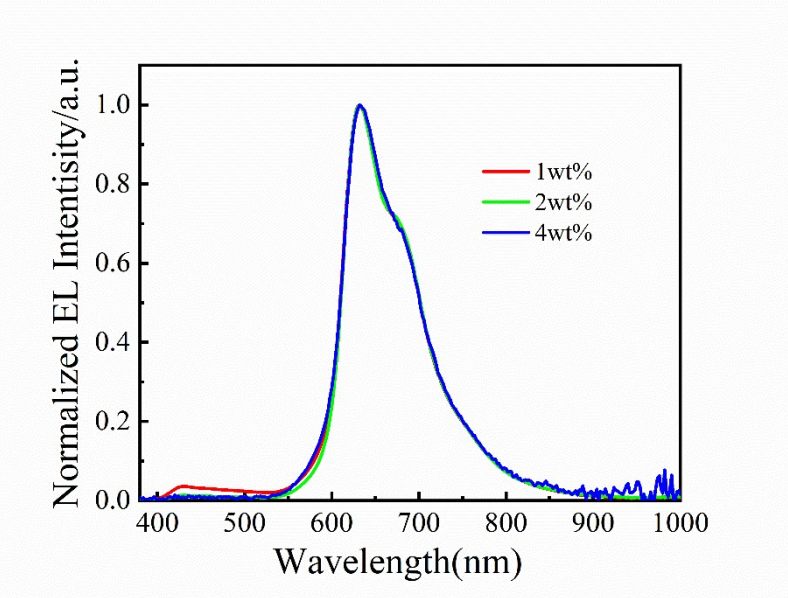

Figure S9. EL spectra of (BIQPy)Pt(DPM)$_2$ doped devices at various concentrations from 1 to 4 wt %.

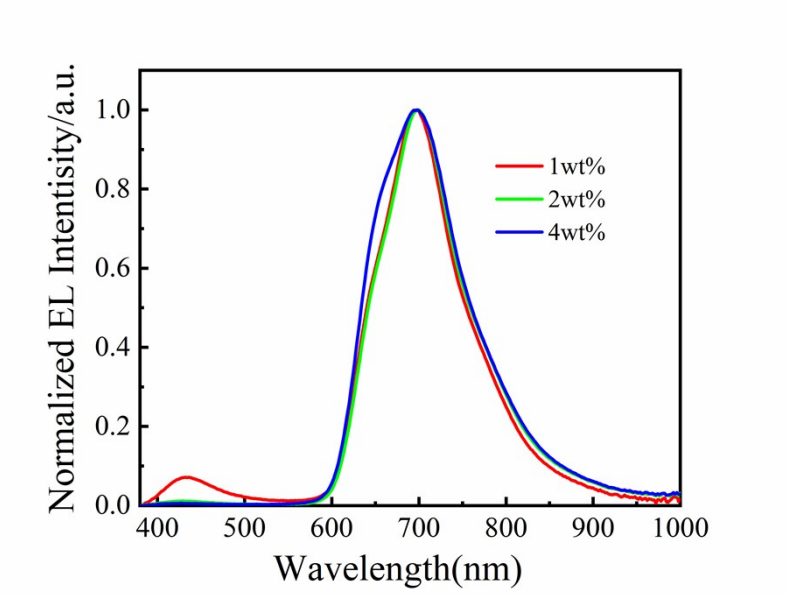

Figure S10. EL spectra of (BIQPy)[Pt(DPM)]$_2$ doped devices at various concentrations from 1 to 4 wt %.

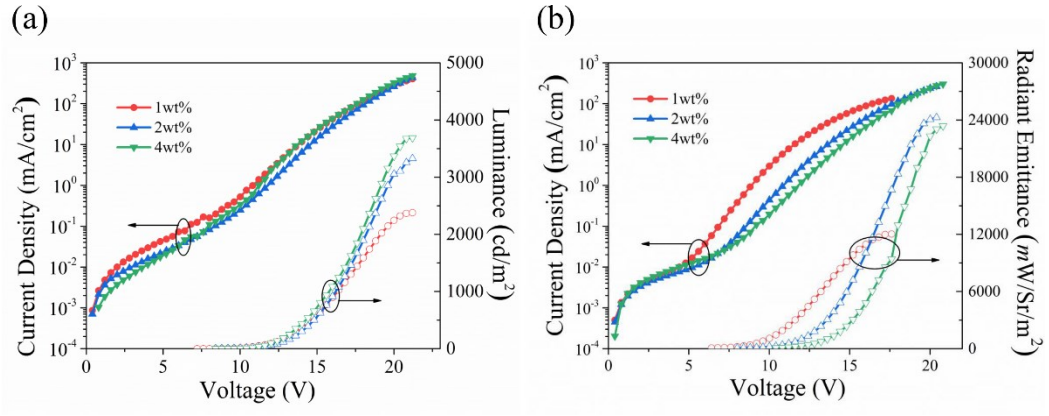

Figure S11. *J–V–R* profiles of platinum(Ⅱ) complexes doped devices at various concentrations from 1 to 4 wt %.

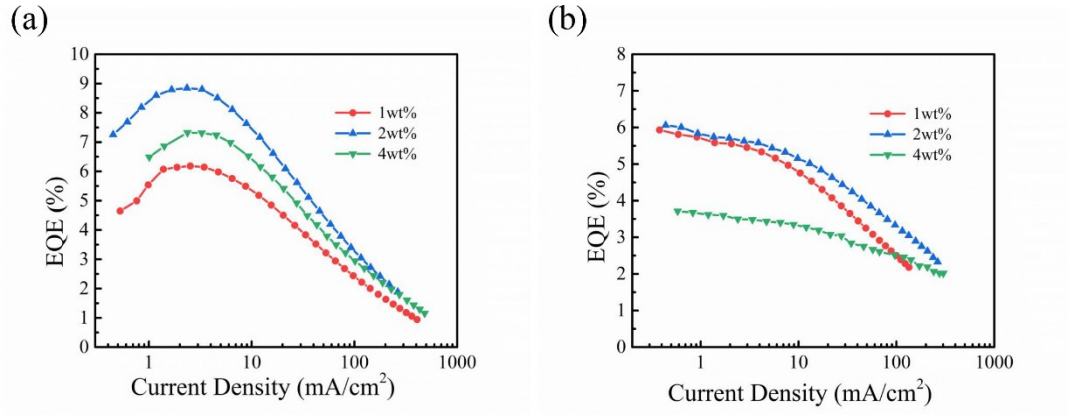

Figure S12. *EQE-J* characteristics of platinum(Ⅱ) complexes doped devices at various concentrations from 1 to 4wt %.

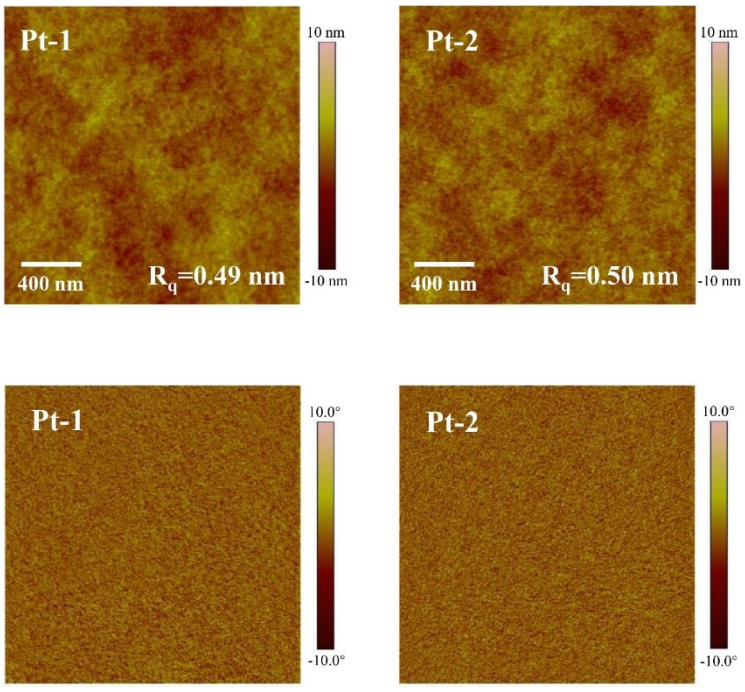

Figure S13. Atomic force microscopy (AFM) measurement of the two complexes based on emissive blends at concentrations of 2 wt %. Height images (top) and phase images (bottom) (2 μm × 2μm), (BIQPy)Pt(DPM) and (BIQPy)[Pt(DPM)]$_2$ replaced with Pt-1 and Pt-2, respectively.

Table S1. Crystal data and refinement parameters for (BIQPy)[Pt(DPM)]$_2$.

Sample	(BIQPy)[Pt(DPM)]$_2$
Empirical formula	$C_{56}H_{56}N_2O_4Pt_2$
Formula weight	1211.20
Temperature/K	170
Crystal system	monoclinic
Space group	$P2_1/c$
a/Å	19.4459(11)
b/Å	9.2887(5)
c/Å	28.9527(16)
α/°	90
β/°	92.182(2)
γ/°	90
Volume/Å^3	5225.9(5)
Z	4
ρ_{calc}g/cm^3	1.539
μ/mm^{-1}	5.392
F(000)	2376.0
Crystal size/mm^3	0.12 × 0.08 × 0.05
Radiation	MoKα (λ = 0.71073)
2Θ range for data collection/°	4.192 to 52.074
Index ranges	-23 ≤ h ≤ 24, -10 ≤ k ≤ 11, -32 ≤ l ≤ 35
Reflections collected	35423
Independent reflections	10167 [R_{int} = 0.0657, R_{sigma} = 0.0662]
Data/restraints/parameters	10167/50/619
Goodness-of-fit on F^2	1.035
Final R indexes [I>=2σ (I)]	R1 = 0.0370, wR2 = 0.0754
Final R indexes [all data]	R1 = 0.0609, wR2 = 0.0903
Largest diff. peak/hole / e Å^{-3}	1.32/-1.41

Table S2. Excited state properties of (BIQPy)Pt(DPM) (Pt-1) and(BIQPy)[Pt(DPM)]$_2$ (Pt-2) obtained from TD-DFT calculations carried out at the ground state(S_0) geometry.

Complex	State（E, λ）	Dominant excitations	Oscillator strength	Character
Pt-1	S_1 (2.18eV, 568nm)	HOMO→LUMO(97.87)	0.038	ILCT/MLCT/LE
	S_2 (2.93eV, 422nm)	HOMO-1→LUMO(79.42) HOMO→LUMO+2(6.70)	0.1415	ILCT/LE/LLCT LLCT/ILCT
	S_3 (2.99eV, 413nm)	HOMO→LUMO+1(92.80)	0.0140	ILCT/MLCT/LLCT
	S_4 (3.05eV, 407nm)	HOMO→LUMO+2(85.69) HOMO→LUMO+3(7.23)	0.0524	LLCT/ILCT LE/ILCT
	S_5 (3.15eV, 393nm)	HOMO-4→LUMO(90.88) HOMO-3→LUMO(4.33)	0.0028	MLCT/MC LE/ILCT/LLCT
	T_1 (1.89eV, 655nm)	HOMO-1→LUMO(4.31) HOMO→LUMO(87.26)	triplet	ILCT/LE/LLCT ILCT/MLCT/LE
	T_2 (2.02eV, 612nm)	HOMO-1→LUMO(13.96) HOMO→LUMO(7.07) HOMO→LUMO+2(10.75) HOMO→LUMO+3(45.29) HOMO→LUMO+4(9.23)	triplet	ILCT/LE/LLCT ILCT/MLCT/LE LLCT/ILCT LE/ILCT ILCT/LLCT/LE
	T_3 (2.32eV, 534nm)	HOMO-3→LUMO(10.75) HOMO-2→LUMO(10.68) HOMO-1→LUMO(40.75) HOMO→LUMO+3(14.01)	triplet	LE/ILCT/LLCT LLCT/LE ILCT/LE/LLCT LE/ILCT
	T_4 (2.60eV, 477nm)	HOMO-3→LUMO(5.07) HOMO-3→LUMO+1(20.68) HOMO-2→LUMO+1(6.78) HOMO-1→LUMO+1(34.07)	triplet	LE/ILCT/LLCT LE/LMCT LE/LLCT/MLCT LE/ILCT
	T_5 (2.77eV, 447nm)	HOMO-3→LUMO+2(5.87) HOMO-2→LUMO+2(25.20) HOMO→LUMO+1(13.63) HOMO→LUMO+2(27.70) HOMO→LUMO+3(5.63)	triplet	LE/LLCT/MLCT LE/MLCT ILCT/MLCT/LLCT LLCT/ILCT LE/ILCT
Pt-2	S_1 (1.83eV, 677nm)	HOMO→ LUMO(98.50)	0.0442	ILCT/LE/MLCT
	S_2 (2.16eV, 575nm)	HOMO→ LUMO+1(98.25)	0.0008	ILCT
	S_3 (2.79eV, 445nm)	HOMO-1→ LUMO(85.61) HOMO→ LUMO+2(7.58)	0.2321	LE/ILCT/LLCT LE/ILCT
	S_4 (2.96eV, 419nm)	HOMO-4→ LUMO(7.50) HOMO-2→ LUMO(74.67) HOMO→ LUMO+4(11.71)	0.0017	MLCT ILCT/LLCT ILCT/LLCT
	S_5 (2.97eV, 418nm)	HOMO→ LUMO+2(16.86) HOMO→ LUMO+3(80.83)	0.0123	LE/ILCT LLCT/ILCT
	T_1 (1.55eV, 801nm)	HOMO→ LUMO(96.06)	triplet	ILCT/LE/MLCT
	T_2 (1.91eV, 648nm)	HOMO-1→ LUMO(23.90) HOMO→ LUMO+2(40.48)	triplet	LE/ILCT LE/ILCT

		HOMO→ LUMO+3(8.90)		LLCT/ILCT
	T_3 (1.97eV, 631nm)	HOMO→ LUMO+1(90.49)	triplet	ILCT
	T_4 (2.26eV, 548nm)	HOMO-4→ LUMO+1(8.95) HOMO-1→ LUMO(49.33) HOMO→ LUMO+2(19.40)	triplet	MLCT LE/ILCT LE/ILCT
	T_5 (2.32eV, 534nm)	HOMO-4→ LUMO(34.19) HOMO-1→ LUMO+1(37.80)	triplet	MLCT LE/LLCT